The preparation of the complexes **1**,[27] **2**,[28] **3**,[29] **4**, and **5**[28] was carried out following the procedure of Reynolds and Wilkinson.[30] Analytically pure products were obtained in yields of 60–70% by high vacuum sublimation (80–130 °C).

For the preparation of **2a** (and **4a**), $Na(CH_3C_5H_4)$ was replaced by $Na(CD_3C_5H_4)$ (**6**): 3.0 mL (47.6 mmol) of CD_3I (Fluka, 99% deuteriation) was added dropwise under stirring at −15 to −20 °C to a solution of 4.4 g (50 mmol) of $Na(C_5H_5)$ in 100 mL of THF. After 1 h the mixture was exposed to room temperature and the resulting $CD_3C_5H_5$ (together with the solvent) condensed into a flask cooled by liquid N_2 (pressure: ca. 1300 Pa). Sodium sand (1.4 g, 61 mmol) was added at room temperature and stirred over 12 h. After filtration (G3 frit), solvent evaporation, and drying of the residue at the high vacuum (3 h, 80 °C), all THF was removed. Yield of pure **6**: 3.6 g (72.5%).

(27) Strohmeier, W.; Landsfeld, H.; Gernert, F.; Langhäuser, W. *Z. Anorg. Allg. Chem.* **1961**, *307*, 120.
(28) Jahn, W. Doctoral Dissertation, Universität Hamburg, 1983, p 124.
(29) (a) Burns, J. H.; Baldwin, W. H.; Fink, F. H. *Inorg. Chem.* **1974**, *13*, 1916. (b) Crease, A. E.; Legzdins, P. *J. Chem. Soc., Dalton Trans.* **1973**, 1501.
(30) Reynolds, L. T.; Wilkinson, G. *J. Inorg. Nucl. Chem.* **1959**, *9*, 86.
(31) Eggers, S. H.; Kopf, J.; Fischer, R. D. *Acta Crystallogr., Sect. C: Cryst. Struct. Commun.* **1987**, *C43*, 2288.

Acknowledgment. R.D.F. and H.B. are grateful for financial support by the Deutsche Forschungsgemeinschaft, D.F.G. (Bonn).

Registry No. **1**, 99080-23-6; **2**, 78869-44-0; **2a**, 114928-58-4; **3**, 39470-13-8; **4**, 114928-57-3; **5**, 74858-41-6; $Na(CD_3C_5H_4)$, 114862-55-4; CD_3I, 865-50-9; $Na(C_5H_5)$, 4984-82-1.

Electronic Structure of Metal Dimers. Photoelectron Spectra and Molecular Orbital Calculations of Dicarbonyl- and Dinitrosyl-Bridged Cobalt, Rhodium, and Iridium Cyclopentadienyl Dimers

Greg L. Griewe and Michael B. Hall*

Department of Chemistry, Texas A&M University, College Station, Texas 77843-3255

Received August 17, 1987

Gas-phase, ultraviolet photoelectron spectra, and molecular orbital calculations are reported for $Cp^*_2M_2(\mu\text{-}CO)_2$ ($Cp^* = C_5(CH_3)_5$; M = Co, Rh, Ir) and $Cp_2M_2(\mu\text{-}NO)_2$ (Cp = C_5H_5; M = Co, Rh). Comparison between series of calculations and series of spectra enable us to reassign the "frontier" region of the spectra as well as more thoroughly assign the "metal" and "cyclopentadienyl" regions of the spectra. Our results suggest that the two lowest energy ionizations, which occur from frontier orbitals of b_g and b_u symmetry, reverse their order in the dicarbonyl-bridged Co dimer relative to the dicarbonyl-bridged Rh and Ir dimers. Although others have suggested that $Cp_2Co_2(NO)_2$ has a triplet ground state, our spectra rule out this possibility for both $Cp_2Co_2(NO)_2$ and $Cp_2Rh_2(NO)_2$. Also discussed is the correlation of molecular orbital theory and valence bond theory in the description of the interfragment bonding in these dimers. Only by counting 5σ carbonyl to metal donations and metal to 2π carbonyl donations as contributing to metal–metal bonds can we arrive at the formal single and double metal–metal bonds required by the 18-electron rule for these dimers. Overlap populations suggest weak metal–metal bonds and strong metal–bridging ligand bonds for all of these dimers.

Introduction

The electronic structure of dibridged transition-metal dimers of the type $(C_5R_5)_2M_2(\mu\text{-}CO)_x(\mu\text{-}NO)_{2-x}$ (R = H or CH_3, henceforth Cp and Cp*, respectively; M = Fe, Co, Ni) has received a lot of attention in recent years. These dimers provide good models for experimental and theoretical studies of metal–metal and metal-bridging π acid interactions.

In spite of the volume of work existent there remain unanswered questions about the electronic structures of dimers doubly bridged by π acids. Although investigators agree that metal–bridging ligand interactions are more important than metal–metal interactions in stabilizing these types of dimers,[1] there exists no consensus on the extent of metal–metal bonding. Studies employing photoelectron (PE) spectroscopy and extended Hückel calculations of nitrosyl- and carbonyl-bridged cobalt, rhodium, and nickel dimers reported no evidence of metal–metal bonding.[2,3]

Another issue that needs to be more thoroughly addressed is the correlation of valence bond theory with molecular orbital theory in the description of metal–metal and metal–bridging ligand bonding in these dibridged binuclear complexes. The 18-electron rule requires that metal dimers with 34 (d^9–d^9), 33 (d^8–d^9), or 32 (d^8–d^8) electrons should have metal–metal bond orders of 1.0, 1.5, or 2.0, respectively. Crystallographic studies, however, have demonstrated that all dimers of this series, with the exception of $Cp_2Ni_2(CO)_2$, are isostructural, featuring planar $M_2(CO)_x(NO)_{2-x}$ cores and metal–metal bond distances insensitive to changes in formal metal–metal bond order.[4]

(1) (a) Mitscher, A.; Rees, B.; Lehman, M. S. *J. Am. Chem. Soc.* **1978**, *100*, 3390. (b) Benard, M. *J. Am. Chem. Soc.* **1978**, *100*, 7740. (c) Benard, M. *Inorg. Chem.* **1979**, *18*, 2782. (d) Heijser, W.; Baerends, E. J.; Ros, P. *Farday Symp. Chem. Soc.* **1980**, *No. 14*, 211. (e) Jemmis, E. D.; Pinhas, A. R.; Hoffmann, R. *J. Am. Chem. Soc.* **1980**, *102*, 2576. (f) Granozzi, G.; Tondello, E.; Benard, M.; Fragala, I. *J. Organomet. Chem.* **1980**, *194*, 83.
(2) Granozzi, G.; Casarin, M.; Ajo, D.; Osella, D. *J. Chem. Soc., Dalton Trans.* **1982**, 2047.
(3) Dudeney, N.; Green, J. C.; Kirchner, O. N.; Smallwood, F. S. J. *J. Chem. Soc., Dalton Trans.* **1984**, 1883.

0276-7333/88/2307-1923$01.50/0

Previous PE studies disagree as to the order of the frontier orbitals.[2,3] There also has been no detailed analysis of the bands arising from the t_{2g}-like and e_1 (M–Cp π bonding) orbitals. Very recently the PE spectra of $Cp_2Co_2(CO)_x(NO)_{2-x}$ (x = 0, 1) were reported and interpreted by using discrete variational Xα calculations based on bent and planar core models of $Cp_2Co_2(NO)_2$.[5]

While our work was in progress, Schugart and Fenske[6] reported Fenske–Hall molecular orbital calculations[7] on $Cp_2M_2(CO)_x(NO)_{2-x}$ (M = Fe, Co, x = 0; M = Co, Ni, x = 2). They found that the ordering of the molecular orbitals depends primarily on metal–bridging ligand and not on metal–metal interactions. More recent ab initio calculations of $Cp_2Co_2(NO)_2$ report that the triplet state may be the ground state for the planar conformer.[8]

This study will examine the bonding in dicarbonyl- and dinitrosyl-bridged cobalt, rhodium, and iridium dimers using gas-phase, ultraviolet He I PE spectroscopy and Fenske–Hall calculations.[7] The PE spectra of $Cp^*_2Ir_2(CO)_2$ and $Cp_2Rh_2(NO)_2$ have not been previously reported. Our spectra of the three dimers reported previously[3,5] match the reported spectra and are included for the sake of comparison with our other spectra. The PE spectra will be interpreted by observing trends and comparing the spectra with parameter-free molecular orbital calculations. The enhanced definition of the spectra of the rhodium- and especially the iridium-containing dimers yields a more detailed understanding of the bonding in these dimers.

Experimental Section

The preparation and purification of $Cp^*_2Co_2(CO)_2$,[9] $Cp^*_2Rh_2(CO)_2$,[10] $Cp_2Co_2(NO)_2$,[11] and $Cp_2Rh_2(NO)_2$[12] are from published procedures. $Cp^*_2Ir_2(CO)_2$ was generously provided by Professor W. A. G. Graham. The ultraviolet PE spectra were recorded on a Perkin-Elmer Model PS-18 spectrometer. The total spectra were recorded as single slow scans with the argon $^2P_{3/2}$ and $^2P_{1/2}$ lines at 15.76 and 15.94 eV, respectively, used as the internal reference. No free spikes due to CO or NO were observed, indicating that all compounds were stable and did not decompose in the spectrometer. The resolution for all spectra was better than 50 meV for the fwhm of the argon $^2P_{3/2}$ peak.

Fenske–Hall molecular orbital calculations[7] were performed on the Department of Chemistry's VAX 11/780 computer. Calculations were performed on $Cp_2M_2(EO)_2$ and CpM (M = Co, Rh; EO = CO, NO). The cobalt basis functions were taken from Richardson et al.[13] and were augmented by 4s and 4p functions with exponents of 2.00. The rhodium basis functions were also taken from Richardson et al.[13] and were augmented by 5s and 5p functions with exponents of 2.20. The carbon, nitrogen, and oxygen functions were taken from the double-ζ functions of Clemnti[14] and reduced to a single-ζ function,[15] except for the p valence functions which were retained as the double-ζ function. An exponent of 1.20 was used for the hydrogen atom. The atomic functions were made orthogonal by the Schmidt procedure. Mulliken population analysis[16] was used to determine both the individual atomic charges and the atomic and CpM fragment orbital populations.

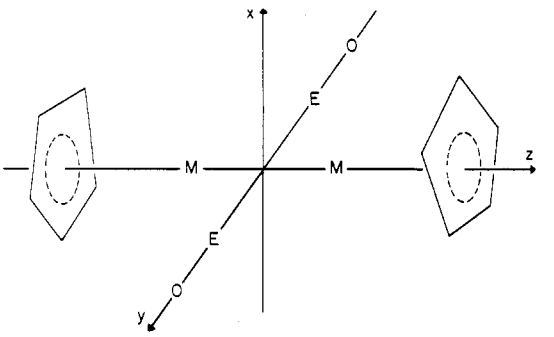

Figure 1. Structure and coordinate system for a planar core model of $(\eta^5\text{-Cp}^*)_2M_2(\mu\text{-EO})_2$ (M = Co, Rh, Ir; EO = CO, NO). The yz plane contains the two metal atoms and both bridging π acids.

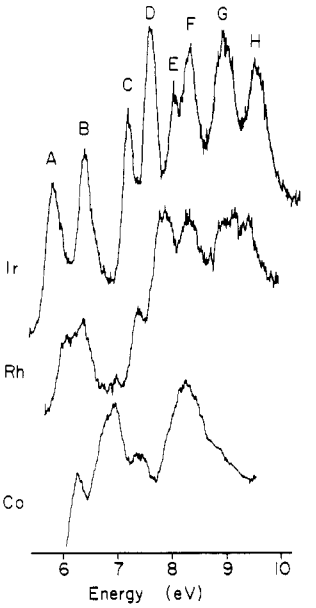

Figure 2. Partial photoelectron spectra for $Cp^*_2M_2(CO)_2$ (M = Co, Rh, Ir).

The molecular geometry for $Cp_2Co_2(EO)_2$ (E = CO, NO) was taken from the crystal structure of $Cp_2Co_2(NO)_2$.[4b] The molecular geometry for $Cp_2Rh_2(EO)_2$ (EO = CO,NO) was taken from the crystal structure of $Cp^*_2Rh_2(CO)_2$.[4h] The cyclopentadienyl rings in these planar core models are staggered with respect to one another, and the model geometries were idealized slightly to perfect C_{2h} symmetry. This geometry and coordinate system are shown in Figure 1. A calculation was also performed on a bent core model of $Cp_2Rh_2(NO)_2$ in which the geometry was based on the average of crystal structures of two $Cp_2Ni_2(CO)_2$ isomers.[4e] The symmetry for the bent model was C_{2v} with the cyclopentadienyl rings eclipsed.

We used Koopmans' theorem[17] in the interpretation of the spectra in spite of its well-documented shortcomings[18] because

(4) (a) Calderon, J. L.; Fontana, S.; Frauendorfer, E.; Day, V. W.; Iske, D. A. *J. Organomet. Chem.* **1974**, *64*, C16. (b) Bernal, I.; Korp, J. D.; Reisner, G. M.; Herrmann, W. A. *J. Organomet. Chem.* **1977**, *139*, 321. (c) Schore, N. E.; Ilenda, C. S.; Bergman, R. G. *J. Am. Chem. Soc.* **1977**, *99*, 1781. (d) Bailey, W. I.; Collins, D. M.; Cotton, F. A.; Baldwin, J. C.; Kaska, W. C. *J. Organomet. Chem.* **1979**, *165*, 373. (e) Byers, L. R.; Dahl, L. F. *Inorg. Chem.* **1980**, *19*, 680. (f) Wochner, F.; Keller, E.; Brintzinger, H. H. *J. Organomet. Chem.* **1982**, *236*, 267. (g) Cirjak, L. M.; Ginsberg, R. E.; Dahl, L. F. *Inorg. Chem.* **1982**, *21*, 940. (h) Green, M.; Hankey, D. R.; Howard, J. A. K.; Louca, P.; Stone, F. G. A. *J. Chem. Soc., Chem. Commun.* **1983**, 757.

(5) Pilloni, G.; Zecchin, S.; Casarin, M.; Granozzi, G. *Organometallics* **1987**, *6*, 597.

(6) Schugart, K. A.; Fenske, R. F. *J. Am. Chem. Soc.* **1986**, *108*, 5094.

(7) Hall, M. B.; Fenske, R. F. *Inorg. Chem.* **1972**, *11*, 768.

(8) Demuynck, J.; Mougenot, P.; Benard, M. *J. Am. Chem. Soc.* **1987**, *109*, 2265.

(9) Dudeney, N.; Green, J. C.; Grebenik, P.; Kirchner, O. N. *J. Organomet. Chem.* **1983**, *252*, 221.

(10) Aldridge, M. L.; Green, M.; Howard, J. A. K.; Pain, G. N.; Porter, S. J.; Stone, F. G. A.; Woodward, P. *J. Chem. Soc., Dalton Trans.* **1982**, 1333.

(11) Becker, P. N.; Bergman, R. G. *Organometallics* **1983**, *2*, 787.

(12) Dimas, P. A.; Lawson, R. J.; Shapley, J. R. *Inorg. Chem.* **1981**, *20*, 281.

(13) Richardson, J. W.; Blackman, M. J.; Ranochak, J. E. *J. Chem. Phys.* **1973**, *58*, 3010.

(14) (a) Clementi, E. J. *J. Chem. Phys.* **1964**, *40*, 1944. (b) Clementi, E. J. *IBM J. Res. Dev.* **1965**, *9*, 2.

(15) Fenske, R. F.; Radtke, D. D. *Inorg. Chem.* **1968**, *7*, 479.

(16) Mulliken, R. S. *J. Chem. Phys.* **1955**, *23*, 1833, 1841.

(17) Koopmans, T. *Physica* (Utrecht) **1934**, *1*, 104.

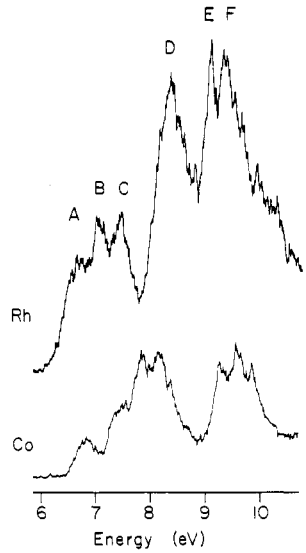

Figure 3. Partial photoelectron spectra for $Cp_2M_2(NO)_2$ (M = Co, Rh).

it is convenient to describe ionizations in terms of the molecular orbitals in the ground-state neutral molecule. Koopmans' theorem is an adequate approximation if the errors it introduces (which are due to relaxation and spin–orbit effects) are relatively constant. Even if it is not exact, it forms a useful approximation as long as the reader understands that our description of the character of ionic states is approximate.

The complete analysis of the spectra of molecules containing third-row transition metals should take into account spin–orbit coupling. Detailed spin–orbit coupling treatments have been used to interpret the PE spectra of mononuclear third-row transition-metal complexes.[19] However, the spectrum of the iridium-containing dimer does not warrant a detailed spin–orbit analysis. Therefore, we used only qualitative spin–orbit arguments to describe the primarily metal ionizations in the spectra.

Results

Photoelectron Spectra. The ionization energy (IE) range of interest for both the dicarbonyl- and dinitrosyl-bridged spectra spans the range 5–11 eV. The IE region of the spectra above 11 eV will not be discussed because of the normally broad and poorly resolved bands due to ionizations from ligand-based orbitals. The partial photoelectron spectra of $Cp^*_2M_2(CO)_2$ (M = Co, Rh, Ir) and $Cp_2M_2(NO)_2$ (M = Co,Rh) are shown in Figures 2 and 3, respectively.

The spectra in both sets of dimers contain three recognizable regions, namely, the "frontier" region (bands A and B in spectrum of $Cp^*_2Ir_2(CO)_2$), the "metal" region (bands C–F in $Cp^*_2Ir_2(CO)_2$) and the "cyclopentadienyl" region (bands G and H in $Cp^*_2Ir_2(CO)_2$). Two general features of these spectra that are especially noticeable in the spectra in Figure 2 are the greater number of distinct ionization bands and the larger separation between the frontier and cyclopentadienyl regions of the spectra as one progresses from Co- to Rh- and to Ir-containing homologues.

In the dicarbonyl-bridged spectra (Figure 2), the Ir "frontier" bands A and B merge in the Rh spectrum forming a broad band and then appear to separate in to a single defined band and a low-energy shoulder on the primary "metal" band in the Co spectrum. "Metal" band C is distinct only in the Ir and Rh spectra. "Metal" bands D and E, which are split in the Ir spectrum, merge in the Rh spectrum and merge with band C to form the larger band in the "metal" region of the Co spectrum. "Metal" band F remains distinct in the Ir, Rh, and Co spectra. Bands G and H, the "cyclopentadienyl" bands, are only distinct in the Ir and Rh spectra.

Unfortunately only the rhdoium- and cobalt-containing dinitrosyl dimers are known. The "frontier" region in the dinitrosyl-bridged Rh complex clearly consists of three bands A–C in Figure 3. In the Co spectrum band A remains distinct, but bands B and C appear to be low-energy shoulders on "metal" ionizations.

The ionization energies and band assignments for the dicarbonyl- and dinitrosyl-bridged dimers are given in Tables I and II, respectively. The explanation of the band assignments will be given in the Discussion.

Table I. Absolute Values for Ionization Energy Peak Maxima (eV) for $Cp^*_2M_2(\mu\text{-}CO)_2$ (M = Co, Rh, Ir)

band	assignmt	ionizatn energies[a] Ir	Rh	Co
A	$3b_g$	5.83	6.09	6.72
B	$4b_u$	6.41	6.40	6.26
C	$3b_u$	7.21	7.37	6.92
D	$4a_g$, $(2b_u - 3a_u)$	7.60	7.83	6.92
E	$(2b_u + 3a_u)$	8.05	7.83	6.92
F	$3a_g$, $2b_g$	8.32	8.21	7.44
G	$2a_g$, $1b_g$, $2a_u$	8.93	8.90	8.25
H	$1b_u$	9.53	9.28	8.25

[a] Estimated error ±0.05 eV.

Table II. Absolute Values for Ionization Energy Peak Maxima (eV) for $Cp_2M_2(\mu\text{-}NO)_2$ (M = Co, Rh)

band	assignmt	ionizatn energies[a] Rh	Co
A	$5a_g$	6.76	6.96
B	$4b_u$	7.14	7.54
C	$3b_g$	7.57	7.95
D	$2b_u$, $3a_g$, $2b_g$ $3a_u$, $4a_g$, $3b_u$	8.33	8.14
E	$2a_u$	9.15	9.60
F	$1b_u$, $1b_g$, $2a_g$	9.39	9.60

[a] Estimated error ±0.05 eV.

Molecular Orbital Calculations. The molecular orbitals of these dimers are perhaps most easily described by using fragment analysis. These dimers will be viewed as formed from two CpM fragments and two bridging π acids.

The 11 lowest lying valence orbitals of the CpM fragments are all localized on the Cp ring contain, virtually no metal character, and are, therefore, unable to participate in dimer bonding. The lowest lying π acid valence orbitals 3σ, 4σ and 1π also do not contribute much to dimer bonding. None of these low-lying orbitals on the CpM and EO fragments will be discussed further.

The orbitals of the CpM fragments pertinent to interpretation of the spectra and bonding for these compounds are $1e_1$, $1e_2$, $1a_1$, $2e_1$, and $2a_1$. The symmetry labels correspond to the C_{5v} symmetry of the CpM fragments. The most stable of the fragment orbitals, the $1e_1$ orbitals, are metal–cyclopentadienyl π bonding and are composed primarily of carbon p_z orbitals. The small metal contribution to the $1e_1$ orbitals comes from the metal d_{yz} and d_{xz} orbitals. The next three orbitals, $1e_2$ and $1a_1$, correspond to the t_{2g} orbitals in an octahedral system. The $1e_2$ is composed of $d_{x^2-y^2}$ and d_{xy} metal orbitals and $1a_1$ is composed of a d_{z^2} metal orbital. The small gap between

(18) (a) Evans, S.; Guest, M. F.; Hillier, I. H.; Orchard, A. F. *J. Chem. Soc., Faraday Trans.* **1974**, *70*, 417. (b) Coutiere, M.; Demuynck, J.; Veillard, A. *Theor. Chim. Acta* **1972**, *27*, 281.

(19) (a) Hall, M. B. *J. Am. Chem. Soc.* **1975**, *97*, 2057. (b) Lichtenberger, D. L.; Fenske, R. F. *J. Am. Chem. Soc.* **1976**, *98*, 50.

Table III. Atomic Composition of CpRh Fragment Orbitals

orbital	% atomic compositn			
	Rh 4d	Rh 5s	Rh 5p	Cp
$2a_1$	1	66	32	1
$2e_1$	65		10	25
$1a_1$	93	5	1	1
e_2	97			3
$1e_1$	28		1	71

$1e_2$ and $1a_1$ arises from weak cyclopentadienyl–metal "δ" bonding interactions stabilizing $1e_2$ as well as the destabilization of $1a_1$ by the mixing in of a small amount of ring character, which is metal–ring "σ*" in the $1a_1$. The next two orbitals, $2e_1$, correspond to the e_g orbitals of an octahedral system. They are the cyclopentadienyl–metal "π" antibonding counterparts of $1e_1$. They are composed primarily of metal d_{xz} and d_{yz} orbitals, but mixing of metal p_x and p_y hybridizes the d_{xz} and d_{yz} orbitals away from the cyclopentadienyl ligand. At even higher energy is the $2a_1$ orbital, which is composed primarily of metal s character hybridized with metal p_z character away from the cyclopentadienyl ring. The atomic characters for the CpRh fragment orbitals, which are very similar to CpCo fragment orbitals, are given in Table III.

Consistent with the notion of larger crystal field splittings expected for second- or third- than for first-row ligated transition metals,[20] the splittings between the CpRh fragment orbitals are larger than those between the CpCo fragment orbitals. The "t_{2g}–e_g" splitting for CpRh is 3.9 eV, 1.0 eV larger than for a CpCo fragment.

The $Cp^*_2M_2(EO)_2$ dimer formation will be described in terms of the higher energy orbitals of the two CpM fragments and the 5σ and 2π orbitals of the bridging π acids. The molecular orbital bonding scheme for the formation of dimers from the fragments is shown in Figure 4. Because there is little mixing among CpM fragment orbitals and the energies of the molecular orbitals reflect the energies of their parent fragments, the molecular orbitals derived from the t_{2g}-like fragment orbitals are energetically distinct from the molecular orbitals derived from the $2e_1$ or $1e_1$ fragment orbitals. The fragment composition of the molecular orbitals of $Cp_2Rh_2(CO)_2$ and $Cp_2Rh_2(NO)_2$ are given in Table IV.

The CpM fragment contribution to $3b_g$, $4b_u$, and $5a_g$, the frontier molecular orbitals, is primarily from the $2e_1$ orbitals. The $5a_g$ is the HOMO for the dinitrosyl-bridged species, and $4b_u$, which is nearly degenerate with $3b_g$ in $Cp_2Rh_2(CO)_2$, is the HOMO for the dicarbonyl-bridged dimers. All three orbitals have strong π metal–metal interactions. The metal–metal interactions of $4b_1$ and $5a_g$ are in the *xz* plane, perpendicular to the molecular-bridging plane, and are metal–metal bonding and antibonding, respectively. The $3b_g$ is in the plane of the bridging ligands (*yz* plane) and is metal–metal antibonding. In both $4b_u$ and $3b_g$ there is back-bonding from the CpM fragments to the bridging ligand 2π orbitals, whereas in the $5a_g$ local symmetry precludes any interaction between the metal fragments and bridging ligands. The fourth molecular orbital derived from the $2e_1$ fragment orbitals is of a_1 symmetry and has metal–metal bonding in the plane of the bridging ligands. This orbital, however, is unfilled because it is strongly destabilized by antibonding interactions with the bridging ligand 5σ orbitals.

The next six molecular orbitals, $3a_g$–$3b_u$, are derived from $1e_2$ and $1a_1$, the t_{2g}-like fragment orbitals, and are almost all metal in character. Molecular orbitals $3a_g$ and $3b_1$ are the metal–metal σ and σ* combinations, respectively, of fragment orbital $1a_1$. The antibonding interaction in $3b_u$ is reduced by fragment orbital $2a_1$ mixing into $3b_u$. Thus, the $3b_u$ has antibonding metal–metal $2a_1$–$2a_1$ and $1a_1$–$1a_1$ interactions but bonding $1a_1$–$2a_1$ interactions. The $2b_g$ and $4a_g$ are the δ and $2b_u$ and $3a_u$ are the δ* combinations of the $1e_2$ fragment orbitals. Fragment orbital $2a_1$ also mixes into $4a_g$, increasing the metal–metal bonding interaction. The $2b_g$ and especially $2b_u$ contain significant amounts of bridging ligand 5σ character.

The next set of molecular orbitals, $1b_u$–$2a_u$, is derived from the $1e_1$ fragment orbitals and contains mainly ring character. The last set of molecular orbitals shown in Figure 4, $1a_u$ and $1a_g$, are derived primarily from the 5σ bridging ligand orbitals. These bridge-based molecular orbitals also contain metal fragment character. Metal fragment orbitals $1a_1$ and $2a_1$ contribute to $1a_g$, and fragment orbitals $1e_1$ and $2e_1$ contribute to $1a_u$.

Substitution of metals or bridging ligands in these dimers produces easily explained changes in the molecular orbital interaction scheme. Substitution of Co for Rh in these dimers decreases the energy gap between groups of molecular derived from different sets of fragment orbitals, reflecting the smaller fragment orbital separation in first-row transition-metal fragments. A subtler change is the stabilization of molecular orbital $3b_g$ relative to $4b_u$ upon substitution of Co for Rh (vide infra).

Substitution of bridging carbonyls with nitrosyls stabilizes molecular orbitals that contain large amounts of

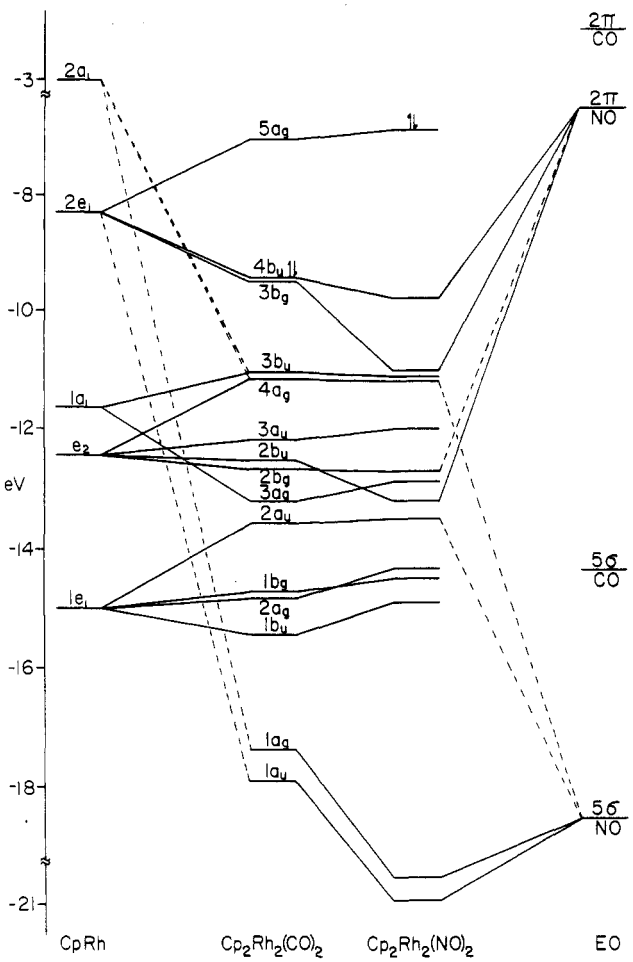

Figure 4. Molecular orbital diagram for $Cp_2Rh_2(EO)_2$ (EO = CO, NO). The energy values were obtained from Fenske–Hall calculations. The dashed lines indicate small but significant contributions from the fragment orbitals to the molecular orbitals.

(20) (a) Figgis, B. N. *Introduction to Ligand Fields*; Wiley-Interscience: New York, 1966. (b) Cotton, F. A.; Wilkinson, G. *Advanced Inorganic Chemistry*, 4th ed.; Wiley-Interscience: New York, 1980.

Table IV. Molecular Composition of $Cp_2Rh_2(\mu\text{-}EO)_2$ (EO = CO, NO)

	fragment composition													
	% $1e_1$		% e_2		% $1a_1$		% $2e_1$		% $2a_1$		% σ EO		% π EO	
orbital	CO	NO	CO	NO	CO	NO	CO	NO	CO	NO	CO	NO	CO	NO
$5a_g$	1	1					99	99						
$4b_u$	6	9					77	57					17	33
$3b_g$	2	9					53	33					43	54
$3b_u$			10	32	70	55			7	7			13	5
$4a_g$			61	71	19	17			12	8	8	3		
$3a_u$			99	99										
$2b_u$			67	45	1	7				2			30	46
$2b_g$			85	81									15	19
$3a_g$			22	16	73	80			2	2	3	1		
$2a_u$	76	89					13	4			10	4		
$1b_g$	93	88						2					6	10
$2a_g$	99	99					1	1						
$1b_u$	90	89					3	6					6	4
$1a_g$			5	3	5	2			10	8	72	83		
$1a_u$	12	5					8	9			76	80		

Table V. Mulliken Overlap Populations for $Cp_2Rh_2(\mu\text{-}EO)_2$ (EO = CO, NO) by Molecular Orbital

	overlap pop.			
	CpRh–RhCp		CpRh–EO	
orbital	CO	NO	CO	NO
$5a_g$		−0.085		0.000
$4b_u$	0.050	0.035	0.017	0.021
$3b_g$	−0.052	0.034	0.028	0.027
$3b_u$	−0.029	−0.030	0.006	0.004
$4a_g$	0.021	0.019	0.011	0.003
$3a_u$	−0.010	−0.010	0.000	0.000
$2b_u$	−0.006	−0.004	−0.001	0.007
$2b_g$	0.008	−0.008	0.001	0.008
$3a_g$	0.064	0.067	−0.005	−0.003
$2a_u$	0.002	0.002	0.008	0.000
$1b_g$	0.005	−0.017	0.003	0.003
$2a_g$	−0.013	−0.016	0.000	0.000
$1b_u$	0.018	0.018	−0.002	0.003
$1a_g$	0.022	0.023	0.025	0.028
$1a_u$	0.013	0.011	0.011	0.018

bridging ligand character. This is seen in orbitals $4b_u$, $3b_g$, and $2b_u$ as well as in the EO-based orbitals $1a_u$ and $1a_g$. In general, the more bridging ligand character an orbital has, the more it is stabilized upon substitution. Of course, the stabilization is just a reflection of the lower energies of the nitrosyl fragment orbitals. Also stabilized, but not shown in Figure 4, are five virtual orbitals. Three of these virtual orbitals are greatly stabilized, causing the HOMO–LUMO gap in $Cp_2Rh_2(NO)_2$ to be only 2.3 eV. The comparable gap in $Cp_2Rh_2(CO)_2$ between $5a_g$ and the next virtual orbital is 6.0 eV. A much smaller change effected by substitution of nitrosyls for carbonyls is the destabilization of molecular orbitals containing little or no bridging ligand character. This destabilization results from the reduction of charge on the CpM fragments, from +0.32 in $Cp_2Rh_2(CO)_2$ to +0.05 in $Cp_2Rh_2(NO)_2$.

As shown in Table V, many molecular orbitals contribute to the bonding between metal fragments and between metal fragments and bridging ligands. Most of the bonding between the metal fragments and the 2π EO orbitals occurs in frontier orbitals $3b_g$ and $4b_u$. Most of the bonding between the metal fragments and the 5σ EO orbitals occurs in orbitals $1a_u$, $1a_g$, and, because of some 4σ–5σ mixing, two more stable orbitals. Significant σ interactions between metal fragments are found in molecular orbitals $1a_g$, $3a_g$, $4a_g$, and $3b_u$. The more important π interactions between the metal fragments are in the frontier orbitals. Weaker metal–metal π interactions are in $1a_u$, $1b_u$, $2a_g$, and $1b_g$.

A clear description of the overall interfragment bonding can be obtained from the population analysis in Table VI. The net overlap population between a metal fragment and an EO fragment is 0.22 in $Cp_2Rh_2(CO)_2$ and $Cp_2Rh_2(NO)_2$. The interaction of the $2a_1$ and $2e_1$ metal fragment orbitals with the EO 5σ (plus some 4σ mixing) and 2π orbitals accounts for nearly all of the CpM–EO bonding. Metal fragment orbitals $1a_1$ and $1e_2$ also make small contributions to CpM–EO bonding. In $Cp_2Rh_2(CO)_2$ the carbonyl 5σ contributions are slightly larger than the 2π contributions to CpM–EO bonding, with CpM–5σ-EO and CpM–2π-EO overlap populations of 0.12 and 0.10, respectively. In $Cp_2Rh_2(NO)_2$, as expected, the 2π nitrosyl contributions to CpM–EO bonding are slightly larger than the 5σ contributions, with CpM–5σ-EO and CpM–2π-EO overlap populations of 0.09 and 0.12, respectively. In both the dicarbonyl- and dinitrosyl-bridged dimers the net overlap population of the metal fragments with the $2\pi_{yz}$ EO orbitals (in-plane) is more than twice as large as than with the $2\pi_{xy}$ EO orbitals (out-of-plane).

The net overlap populations between metal fragments in the dicarbonyl- and dinitrosyl-bridged dimers are 0.056 and −0.059, respectively. Most of the difference in the metal–metal overlap populations arises from filling the $5a_g$, the HOMO in dinitrosyl- and the LUMO in dicarbonyl-bridged dimers. $5a_g$ is strongly metal–metal π antibonding, with an overlap population between the metal fragments of −0.085 in $Cp_2Rh_2(NO)_2$. The σ bonding between the metals is due to the $1a_1$ and $2a_1$ fragment orbitals and accounts for most of the metal–metal bonding. The σ overlap population between metal fragments in $Cp_2Rh_2(CO)_2$ is 0.045. The rest of the metal–metal bonding arises

Table VI. Mulliken Overlap Populations for $Cp_2Rh_2(\mu\text{-}EO)_2$ (EO = CO, NO)

	overlap pop.										
molecule	$1a_1$–$1a_1$	$1a_1$–$2a_1$	$2a_1$–$2a_1$	$2e_1$–$2e_1$	$1e_2$–π	$1a_1$–σ	$2e_1$–σ	$2e_1$–π	$2a_1$–σ	$2a_1$–π	total
$Cp_2Rh_2(CO)_2$											
CpRh–RhCp	0.013	0.070	−0.011	0.032							0.056
CpRh–CO					0.026	0.013	0.066	0.063	0.070	0.016	0.222
$Cp_2Rh_2(NO)_2$											
CpRh–RhCp	0.019	0.071	−0.036	−0.065							−0.059
CpRh–NO					0.028	0.011	0.050	0.063	0.054	0.020	0.217

from the π interactions of the $2e_1$ fragment orbitals.

Discussion

Spectra and Calculations. Usually the relative one-electron energies obtained from Fenske–Hall calculations correlate reasonably well with the observed ionization energies in the PE spectra.[21] Although our calculations were performed on Cp- and not Cp*-containing dimers, one can easily account for the shifts in the energies produced by this change. The reported destabilization of the ring-based orbitals of $Cp^*Co(CO)_2$ relative to $CpCo(CO)_2$ is 1.1 eV.[22] Due to increased electron density on the metals, orbitals composed of metal character are also destabilized, although not as much as ring-based orbitals. The reported destabilization of the metal-based orbitals of $Cp^*Co(CO)_2$ relative to $CpCo(CO)_2$ is 0.6 eV. What we should and do see in these dimers is the destablization of all three upper regions ("frontier", "metal", and "cyclopentadienyl") in the spectra of $Cp^*_2M_2(CO)_2$ compared with $Cp_2M_2(NO)_2$. A more detailed comparison of ionization energies between these two series of spectra is impossible because an all $Cp_2M_2(CO)_x(NO)_{2-x}$ or all $Cp^*_2M_2(CO)_x(NO)_{2-x}$ series of dimers does not exist. The partial PE spectra of $Cp^*_2Co_2(CO)_2$,[3] $Cp^*_2Rh_2(CO)_2$,[3] and $Cp_2Co_2(NO)_2$[5] have already appeared and are included for the sake of comparison. The new spectra, $Cp^*_2Ir_2(CO)_2$ and $Cp_2Rh_2(NO)_2$, provide the key to understanding the electronic structure of these two series.

The dicarbonyl-bridged series of spectra will be discussed first because the well-defined spectrum of $Cp^*_2Ir_2(CO)_2$ facilitates the assignment of the PE bands. The filled frontier orbitals in the dicarbonyl-bridged compounds are $3b_g$ and $4b_u$. $3b_g$ is an in-plane metal–metal π antibonding combination and $4b_u$ is an out-of-plane metal–metal π bonding combination of the CpM fragment $2e_1$ orbitals. Both $3b_g$ and $4b_u$ contain substantial back-bonding from the CpM fragments to the bridging π acids. The observed gap between bands A and B is 0.46, 0.31, and 0.58 eV in the Co, Rh, and Ir spectra, respectively. The calculated gap between $3b_g$ and $4b_u$ is 0.19 eV and 0.04 eV in the Co and Rh $Cp_2M_2(CO)_2$ calculations, respectively. The band assignments consistent with the observed and calculated changes in the frontier orbital gaps are that the first ionization band in the Co dimer corresponds to $4b_u$ (band B) and the first ionization of the Rh and Ir dimers corresponds to $3b_g$ (band A).

The relative energies of $3b_g$ and $4b_u$ depend on the subtle balance of CpM–MCp and CpM–EO interactions. The Rh 4d and Ir 5d atomic orbitals are more diffuse than the Co 3d atomic orbitals allowing the metal–metal interactions to be stronger in the Rh and Ir dimers than in the Co dimer. Obviously, substitution of the metals affects the metal–metal interactions more than metal–bridging ligand interactions, stabilizing $4b_u$ relative to $3b_g$ in the Rh and Ir dimers. Extended Hückel calculations of $Cp_2Co_2(CO)_2$ predicted that $4b_u$ was more stable than $3b_g$.[23] In the previous PE study of $Cp^*_2Co_2(CO)_2$ and $Cp^*_2Rh_2(CO)_2$ these extended Hückel calculations were used to assign the spectra.[3] Consequently, the band of lowest ionization energy in both the Co and Rh spectra was assigned to $3b_g$. The trend from Ir to Rh in the spectra and the trend in the calculations suggest that the $4b_u$ is the correct assignment for the first band in the Co dimer.

Heretofore, the "metal" and "cyclopentadienyl" regions of the PE spectra have not been thoroughly assigned primarily because of inadequate band definition. The PE spectrum of $Cp^*_2Ir_2(CO)_2$ has sufficient definition to allow assignment of bands in the "metal" and "cyclopentadienyl" regions. The "metal" region comprises bands C–F in the dicarbonyl-bridged spectra. The relative intensities of bands C–F suggest that bands D and F are each composed of two orbitals and that bands C and E are each composed of one orbital. This scheme accounts for all molecular orbitals of t_{2g}-like parentage.

Spin–orbit coupling must be taken into consideration in order make band assignments in the "metal" region. The molecular orbitals closest in energy and of the proper composition to have a large spin–orbit matrix element are $2b_u$ and $3a_u$. Our approximate interpretation of the spin–orbit coupling suggests that the destabilized combination of $2b_u$ and $3a_u$ is degenerate with $4a_g$ forming band D, with the stabilized combination forming band E. The gap between bands D and E, 0.45 eV, is a reasonable value for the molecular spin–orbit splitting for an iridium dimer. Our calculations, consistent with the notion that σ metal–metal interactions are much stronger than δ metal–metal interactions, suggest that band C is composed of $3b_u$, the σ^* combination of $1a_1$ fragment orbitals, and that band F is partly composed of $3a_g$, the σ combination of $1a_1$ fragment orbitals. Bands D and E merge in the Rh spectrum and combine with band C in the Co spectrum. Band F remains distinct in all three spectra.

The "cyclopentadienyl" region is composed of bands G and H. The relative intensities of these bands leads us to assign orbitals $2a_g$, $1b_g$, and $2a_u$ to band G and $1b_u$ to band H. Bands G and H are distinct in the Rh and Ir spectra but merge in the Co spectrum.

The spectra of the dinitrosyl-bridged dimers show the same general features as the dicarbonyl-bridged dimers. The major difference is the additional band in the "frontier" region of the d^9–d^9 dimers. The calculated energy gaps between $3b_g$, $4b_u$, and $5a_g$, the three filled frontier orbitals, are relatively large leaving no doubt as to the assignment of the "frontier" bands. The calculated HOMO, $5a_g$, is assigned to the lowest energy ionization, band A. Orbitals $4b_u$ and $3b_g$ are assigned to bands B and C, respectively. There is no ambiguity in the assignment of bands B and C in the dinitrosyl-bridged dimers because of the relatively large difference in the calculated energies of molecular orbitals $4b_u$ and $3b_g$. In the Co spectrum bands B and C are separate shoulders on the low-energy side of the broad "metal" band. The entire "metal" region of the Rh spectrum is contained in band D. However, in the Co spectrum some of the higher lying "metal" orbitals, e.g. $3b_u$ or $4a_g$, may contribute to band C. The "cyclopentadienyl" region of the Rh spectrum is composed of two bands, E and F. There is a shoulder on the high-energy side of band F. The relative intensities of bands E and F suggest that band E is composed of a single orbital, $2a_u$, and that band F is composed of orbitals $1b_g$ and $2a_g$, with perhaps the shoulder of band F composed of $1b_u$. The 1:2:1 intensity pattern of bands E and F and the shoulder, respectively, reflects the intensity pattern of the "cyclopentadienyl" region of the Co spectrum.

The PE spectrum of $Cp^*_2Co_2(NO)_2$ has been reported.[3] Naturally the spectrum is very similar to that of $Cp_2Co(NO)_2$. Their assignment of the "frontier" region of $Cp^*_2Co_2(NO)_2$ switched the energies of the bands assigned

(21) (a) Lichtenberger, D. L.; Fenske, R. F. *Inorg. Chem.* **1976**, *15*, 2015. (b) Block, T. F.; Fenske, R. F. *J. Am. Chem. Soc.* **1977**, *99*, 4321. (c) Hubbard, J. L.; Lichtenberger, D. L. *Inorg. Chem.* **1980**, *19*, 1388. (d) Morris-Sherwood, B. J.; Kolthammer, B. W. S.; Hall, M. B. *Inorg. Chem.* **1981**, *20*, 2771. (e) DeKock, R. L.; Wong, K. S.; Fehlner, T. P. *Inorg. Chem.* **1982**, *21*, 3203.

(22) Lichtenberger, D. L.; Calabro, D. C.; Kellogg, G. E. *Organometallics* **1984**, *3*, 1623.

(23) Pinhas, A. R.; Hoffmann, R. *Inorg. Chem.* **1979**, *18*, 654.

to $3b_g$ and $4b_u$, relative to our assignment, giving the $3b_g$ band a lower ionization energy than the band due to $4b_u$.

The PE spectrum of $Cp_2Co_2(NO)_2$ has also been reported by Pilloni et al.[5] Its spectrum was interpreted by using discrete variational Xα calculations based on bent and planar core models of $Cp_2Co_2(NO)_2$. Their bent core calculations were prompted by the solution IR spectrum of $Cp_2Co_2(NO)_2$, which has two nitrosyl stretching frequencies, indicative of a bent core geometry. A bent-core gas-phase geometry was proposed because the relatively small gap observed between the highest and second highest occupied molecular orbitals in the PE spectrum was better approximated by the calculations based on a bent core model. The total theoretical electron density map shows charge accumulation between the Co atoms, indicative of a direct Co–Co bond, only for the bent core model and not for the planar core model.

Our calculations of $Cp_2Rh_2(NO)_2$, based on the same bent core model as Pilloni et al.,[5] also showed a stabilization of the HOMO relative to the second highest occupied molecular orbital. The calculated gap between these orbitals is 2.88 eV for the planar core model and 1.69 eV for the bent core model, perhaps allowing our bent core model to more closely match the PE spectrum. However, there are several differences between the results of Pilloni et al. and our results. The first is that although our HOMO is stabilized in the bent calculation, the relative stabilization is not as much as reported for $Cp_2Co_2(NO)_2$. Pilloni et al. reported that the HOMO for $Cp_2Co_2(NO)_2$ was stabilized primarily because of reduced Cp–M π antibonding and not due to increased metal–nitrosyl bonding. Our calculations on $Cp_2Rh_2(NO)_2$ found that the HOMO was stabilized by increased metal–nitrosyl bonding as well as reduced Cp–M π antibonding. Instead of finding increased metal–metal bonding in the bent model, as was reported for $Cp_2Co_2(NO)_2$, we found that the overlap population between the metal fragments drops from −0.059 in the planar model to −0.105 in the bent model. On the basis of our calculations and PE spectra we cannot assign a gas-phase geometry to $Cp_2Co_2(NO)_2$ or $Cp_2Rh_2(NO)_2$ with any certainty.

Recently, the possibility of a triplet ground state for the planar conformation of $Cp_2Co_2(NO)_2$ was reported.[8] Our calculations of $Cp_2Co_2(NO)_2$ and $Cp_2Rh_2(NO)_2$ show that both have relatively small HOMO–LUMO gaps (2.4 eV and 2.3 eV, respectively), at least compared to the LUMO–SLUMO (second lowest unoccupied molecular orbital) gaps in the dicarbonyl-bridged species. However, the spectra are inconsistent with a triplet ground state for the dinitrosyl-bridged Co and Rh dimers. A triplet ground state has two open shells. Ejection of an electron from one of the doubly occupied orbitals of a triplet state molecule will produce molecular ions in both doublet and quartet states.[24] Few or all of these states may be observed, thus greatly complicating the PE spectrum. In small molecules one may observe PE spectra with multiple bands arising from each molecular orbital. In large molecules one may observe instead PE spectra with relatively broad, poorly resolved bands. Our spectra, especially the Rh spectrum, have relatively narrow well-defined bands. Even more telling is the lack of the minimum of four "frontier" bands in the dinitrosyl-bridged spectra as required by a triplet ground state for these dimers.

Nature of the Bonding. Our calculations clearly show that metal–bridging ligand interactions are more important than metal–metal interactions in holding these dimers together. This is in agreement with the findings of others,[1-3] who view the interactions in the $M_2(EO)_2$ core as best described as delocalized multicentered bonding.[25] Although overlap populations cannot be used as absolute measurements of bonding, comparisons of overlap populations between closely related bond types can give reasonable estimates of bonding. In both the dicarbonyl- and the dinitrosyl-bridged dimers the overlap population between each CpRh–EO interaction is 0.22. This is large compared to the net CpRh–RhCp overlap populations of +0.06 in the dicarbonyl-bridged and −0.06 in the dinitrosyl-bridged dimers. Of course, because these are dissimilar bond types not too much should be made of this comparison, but it is an indication that metal–bridging ligand interactions dominate the interfragment bonding. As reported for $Cp_2Co_2(EO)_2$ (EO = CO, NO),[6] the 5σ and 2π EO orbitals are roughly equally responsible for bonding with the metal fragments in $Cp_2Rh_2(EO)_2$. The 5σ orbitals are slightly more important in the dicarbonyl- and the 2π are slightly more important in the dinitrosyl-bridged dimers.

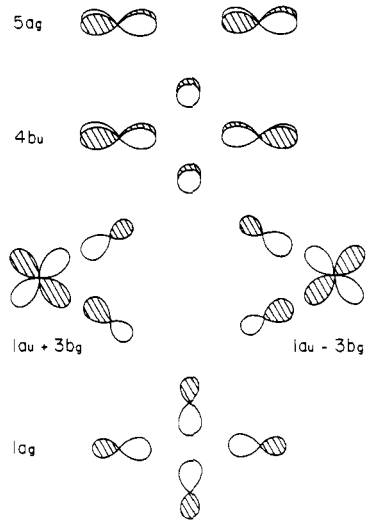

Figure 5. Valence description interfragment bonding. The view is of the *yz* plane (molecular plane). Only orbitals of the metals and proximal atom of the bridging ligands are shown.

Formally, dicarbonyl-bridged, d^8–d^8, dimers have double metal–metal bonds and dinitrosyl-bridged dimers, d^9–d^9, dimers have single metal–metal bonds. For our type of calculation a typical overlap population between two unbridged ruthenium atoms in a single 2c–2e bond is 0.13.[26] The CpRh–RhCp overlap populations in both the dicarbonyl- and dinitrosyl-bridged dimers fall far short of this benchmark overlap population. All that can be said of our CpRh–RhCp overlap populations is that the difference between the overlap populations of the d^8–d^8 and d^9–d^9 dimers is 0.12, reflecting a difference of a bond order between the two dimers.

Alluded to previously, but not explained, is the correlation of valence bond theory to molecular orbital theory in the description of interfragment bonding in these dimers. As an approximation we will focus on the molecular orbitals of $2e_1$ or $2a_1$ CpM parentage and 5σ or 2π EO parentage. Thus, the molecular orbitals that will be used in the valence description are $1a_g$, $1a_u$, $3b_g$, $4b_u$, and $5a_g$. Orbitals $1a_u$ and $3b_g$ both contain metal d_{yz} character. $1a_u$ is the in-phase and $3b_g$ is the out-of-phase combination of

(24) Rabalais, J. W. *Principles of Ultraviolet Photoelectron Spectroscopy*; Wiley: New York, 1977.

(25) (a) Chini, P. *Inorg. Chim. Acta, Rev.* **1968**, *2*, 31. (b) Braterman, P. S. *Struct. Bonding (Berlin)* **1971**, *10*, 57. (c) Mason, R.; Mingos, D. M. P. *J. Organomet. Chem.* **1973**, *50*, 53.

(26) Sherwood, D. E.; Hall, M. B. *Inorg. Chem.* **1982**, *21*, 3458.

the metal d_{yz} orbitals. Linear combinations of $1a_u$ and $3b_g$ can be made in order to emphasize net interactions. Orbitals $1a_g$, $4b_u$, $5a_g$, and the linear combinations of $1a_u$ and $3b_g$ are shown in Figure 5. Of course $1a_u$ and $3b_g$ can be regenerated by adding or subtracting, respectively, the linear combinations illustrated in Figure 5.

According to the 18-electron rule, the formal metal–metal bond orders of the dicarbonyl- and dinitrosyl-bridged dimers are 2.0 and 1.0, respectively. In the dicarbonyl-bridged dimers all orbitals shown in Figure 5 are filled except $5a_g$, the LUMO. The two metal–metal bonds are represented by $1a_g$ and $4b_u$. These are 4c–2e bonds and contain substantial amounts of CpM–EO bonding. The linear combinations of $1a_u$ and $3b_g$ are exclusively CpM–EO bonding. In dinitrosyl-bridged dimers all orbitals are filled, including $5a_g$. The out-of-plane π metal–metal bond in $4b_u$ is more than cancelled by the out-of-plane π^* metal–metal antibond in $5a_g$. Therefore, in dinitrosyl-bridged dimers the only net metal–metal bonding interaction is the in-plane σ bond in $1a_g$. The description given above neglects the $1e_2$ and $1a_1$ fragment orbitals and this t_{2g}-like set is usually believed not to contribute to metal–metal bonding, but as shown in Table VI and in Figure 4, the $1a_1$ fragment orbitals do contribute some additional metal–metal bonding because the bonding in the $3a_g$ is not completely cancelled by their antibonding counterpart, $3b_u$.

Acknowledgment. We thank the Robert A. Welch Foundation (Grant No. A-648) for the support of this work and the National Science Foundation for funds to purchase the VAX 11/780 (Grant No. CHE80-15792). We also thank Professor William A. G. Graham of the University of Alberta for his generous gift of $Cp^*_2Ir_2(CO)_2$.

Registry No. $Cp^*_2Co_2(CO)_2$, 69657-52-9; $Cp^*_2Rh_2(CO)_2$, 69728-34-3; $Cp_2Co_2(NO)_2$, 51862-20-5; $Cp_2Rh(NO)_2$, 67426-08-8; $Cp^*_2Ir(CO)_2$, 106682-38-6.

Low-Valent Rhenium–Oxo–Alkoxide Complexes: Synthesis, Characterization, Structure, and Ligand Exchange and Carbon Monoxide Insertion Reactions[1]

Torsten K. G. Erikson, Jeffrey C. Bryan, and James M. Mayer*

Department of Chemistry, University of Washington, Seattle, Washington 98195

Received October 2, 1987

A series of rhenium(III)–oxo–alkoxide–bis(acetylene) complexes of the form $Re(O)(OR)(R'C{\equiv}CR')_2$ have been prepared by reaction of the iodide derivatives $Re(O)I(R'C{\equiv}CR')_2$ with thallium alkoxides. An X-ray crystal structure of the phenoxide complex **7a** shows the pseudotetrahedral coordination geometry typical of $Re(O)X(RC{\equiv}CR)_2$ compounds, with a short rhenium–oxo bond of 1.712 (13) Å and a longer Re–OPh distance of 1.966 (14) Å. The alkoxide complexes decompose in solution at less than 100 °C by a number of pathways including β-hydrogen elimination. The complexes react rapidly with protic reagents such as alcohols, water, amines, acids, etc. with displacement of alcohol. Reactions of the *tert*-butoxide complex with ammonia or methylamine yield the corresponding amide complexes, and H_2S gives the hydrosulfide species. Many of these ligand exchange reactions give equilibrium mixtures, indicating that the Re–X bond strengths in general parallel H–X bond strengths. The methylamide complex is fluxional on the NMR time scale, with a ground state that places the methyl group pointing at one of the acetylene ligands. The phenoxide ligand in the X-ray structure is approximately in the same sterically encumbered orientation. This orientation is preferred because it favors π-bonding and minimizes π-antibonding interactions of the π-donor orbital of the amide or phenoxide ligand. The ethoxide complex readily inserts carbon monoxide and isopropyl isocyanide to give $Re(O)[C(O)OEt](MeC{\equiv}CMe)_2$ and $Re(O)[C(N\text{-}i\text{-}Pr)OEt](MeC{\equiv}CMe)_2$, respectively. Crystal data for **7a**: $Pna2_1$, a = 18.620 (7) Å, b = 7.2389 (9) Å, c = 10.552 (3) Å, Z = 4, refined to R = 0.044, R_w = 0.044.

We have been studying the chemistry of low-valent rhenium–oxo compounds since our discovery of $Re(O)I(MeC{\equiv}CMe)_2$ (**1a**) in 1984.[2] This compound and its derivatives are remarkable because they contain terminal oxo groups with strong metal–oxygen multiple bonds despite a low formal oxidation state (+3) and a d^4 electron count.[3-5] Compounds with terminal oxo ligands almost always have high oxidation states and d^0, d^1, or d^2 electronic configurations.[6] Previous papers in this series have presented a description of the electronic structure of d^4 oxo–acetylene compounds,[3] discussed their ligand substitution reactions,[7] and described their reduction to di-

(1) Low-Valent Oxo Compounds. 5. For previous papers in this series see ref 2, 3, 7, and 8.
(2) Mayer, J. M.; Tulip, T. H. *J. Am. Chem. Soc.* **1984**, *106*, 3878–9.
(3) Mayer, J. M.; Thorn, D. L.; Tulip, T. H. *J. Am. Chem. Soc.* **1985**, *107*, 7454–7462.
(4) Another d^4 rhenium–oxo compound has recently been described: de Boer, E. J. M.; de With, J.; Orpen, A. G. *J. Am. Chem. Soc.* **1986**, *108*, 8271–3.
(5) For other terminal oxo complexes in d^3 or d^4 configurations, see: Meyer, T. J. et al. *Inorg. Chem.* **1981**, *20*, 436–444; **1983**, *22*, 1407–9; **1984**, *23*, 1845–1851; **1986**, *25*, 3256–3262; *J. Am. Chem. Soc.* **1986**, *108*, 4066–4073. Marmion, M. E.; Takeuchi, K. J. *J. Am. Chem. Soc.* **1986**, *108*, 510–511. Che, C.-M.; Lai, T.-F.; Wong, K.-Y. *Inorg. Chem.* **1987**, *26*, 2289–2299. Aoyagi, K.; Yukawa, Y.; Shimizu, K.; Mukaida, M.; Takeuchi, T.; Kakihana, H. *Bull. Chem. Soc. Jpn.* **1986**, *59*, 1493–1499.
(6) Nugent, W. A.; Mayer, J. M. *Metal.-Ligand Multiple Bonds*; Wiley: New York, in press. Griffith, W. P. *Coord. Chem. Rev.* **1970**, *5*, 459–517.

0276-7333/88/2307-1930$01.50/0